ISSN 0022-0930, Journal of Evolutionary Biochemistry and Physiology, 2021, Vol. 57, No. 6, pp. 1449–1460. © Pleiades Publishing, Ltd., 2021.
Russian Text © The Author(s), 2021, published in Rossiiskii Fiziologicheskii Zhurnal imeni I.M. Sechenova, 2021, Vol. 107, No. 12, pp. 1490–1504.

EXPERIMENTAL PAPERS

Development of Hippocampus-Associated Cognitive Dysfunction in Huntington's Disease Mouse Model

N. A. Kraskovskaya[a,*], A. I. Erofeev[a], E. D. Grishina[a], S. A. Pushkareva[a], E. I. Gerasimov[a], O. L. Vlasova[a], and I. B. Bezprozvanny[a,b,]**

[a] *Peter the Great St. Petersburg Polytechnic University, St. Petersburg, Russia*

[b] *Department of Physiology, UT Southwestern Medical Center at Dallas, Dallas, USA*
**e-mail: ninakraskovskaya@gmail.com*
***e-mail: mnlabspb@gmail.com*

Received September 17, 2021

Revised September 24, 2021

Accepted September 24, 2021

Abstract—Huntington's disease is a hereditary, incurable, neurodegenerative disease characterized by movement disorders—progressive choreic hyperkinesia, as well as cognitive and mental disorders, including memory impairment, depression, panic attacks, obsessive compulsions, etc. According to the literature data, mild cognitive impairments begin to manifest even before the appearance of first motor symptoms. Neurodegeneration of the cortex and striatum is believed to play a major role in the development of cognitive dysfunction. At the same time, pathological changes in the hippocampus, which can also cause cognitive impairments, have been studied to a much lesser extent. In the present study, using electrophysiological experiments, morphofunctional analysis, and behavioral tests, we performed a comprehensive assessment of hippocampus-associated changes in YAC128 transgenic mice which model Huntington's disease. The revealed disturbances in the mechanisms of synaptic plasticity and changes in the morphology of synapses in the hippocampus of YAC128 mice are progressive and occur before motor movement disorders. Thus, the obtained results support the hypothesis of the development of neurodegenerative changes in the hippocampus, which contribute to cognitive dysfunction in Huntington's disease.

DOI: 10.1134/S0022093021060211

Keywords: Huntington's disease, hippocampus, long-term potentiation, dendritic spines, Morris water maze, cognitive impairment, behavioral tests

Abbreviations: HD—Huntington's disease; LTP—long-term potentiation; mHTT—mutant huntingtin; EPSP—excitatory postsynaptic potential; PTP—post-tetanic potentiation

INTRODUCTION

Huntington's disease (HD) is an autosomal dominant, hereditary, incurable neurodegenerative disease. This neuropathology refers to a group of pathologies called trinucleotide repeat expansions that are characterized by triplet multiplication in the regulatory or coding region of genes. In

the case of HD, there is an increase in the CAG repeat encoding the amino acid glutamine in the first exon of the huntingtin protein gene, which leads to the formation of an extended polyglutamine tract in the protein and the development of the HD phenotype [1]. Cognitive and motor disorders in neurodegenerative diseases are associated with morphological and functional changes in the higher parts of the central nervous system (CNS). Although HD is considered a motor disorder [2], patients also exhibit cognitive impairments that appear before motor symptoms [3]. This circumstance indicates that, apart from the striatum, pathological processes in HD also affect other regions of the brain responsible for cognitive functions [4, 5]. In HD, the striatum, cerebral cortex, thalamus and hippocampus are considered the main "foci" of neuropathology. Moreover, the latter is the least studied among all the listed brain regions. Hippocampus-associated cognitive impairments affect memory (particularly spatial), attention, learning ability and memorization of new information. The key to understanding the pathogenesis of degenerative processes that occur in the hippocampus in HD lies in studying the changes in synaptic plasticity and the degradation of synaptic connections of neurons [6]. A stable interneuronal connectivity is maintained by contacts of presynaptic axonal boutons with postsynaptic structures called dendritic spines [7]. However, due to the accumulation of the mutant protein, the number of dendritic spines decrease and results in synaptic dysfunction which eventually leads to cognitive and motor impairments. The development of corticostriatal synaptic dysfunction and the elimination of dendritic spines in cortical and striatal areas in case of HD have been described in detail [8–13]. However, the development of defects in hippocampal synaptic plasticity and their relationship with a reduced number of synapses and behavioral phenotype are hardly studied or studied in such "aggressive" HD mouse models as R6/1 and R6/2 strains with a transgenic insertion carrying only the first exon of the *mHtt* (mutant huntingtin) gene. Their major disadvantage is thought to be the rapid progression of a disease phenotype, while HD, like other neurodegenerative diseases, is an age-related pathology, and the development of its characteristic clinical symptoms begins in adulthood. In this study, the YAC128 mouse strain carrying a transgenic insertion with the full-length human *mHtt* gene was chosen as a HD model. The use of this model enabled better modeling of the age-related phenotype of the disease and by electrophysiological, morphological, and behavioral tests, assessing the progression of hippocampus-associated synaptic dysfunction and cognitive impairments.

MATERIALS AND METHODS

Transgenic animals

The study was carried out on the Tg(YAC128)53Hay-M (abbreviated as YAC128) strain carrying the full-length human huntingtin protein gene within an artificial yeast chromosome. Wild-type (WT) mice of the same background were used as a control. Heterozygous males of the FVB-Tg(YAC128)53Hay/J strain aged 3–6 months were crossed with WT females of the same age. The presence of a transgenic insertion was detected by a polymerase chain reaction with primers to the human huntingtin gene exon 1 (forward primer sequence: 5'-CCG CTC AGG TTC TGC TTT TA-3', reverse primer sequence: 5'-TGG AAG GAC TTG AGG GAC TC-3'). The presence in the sample of a band at a level of approximately 170 base pairs (bp) indicated the presence of a transgenic insertion.

All experimental procedures carried out on the animals complied with the ethical standards approved by the legal acts of the Russian Federation, the principles of the Basel Declaration, and the recommendations of the Bioethics Committee at the Institute of Biomedical Systems and Technologies of the Peter the Great St. Petersburg Polytechnic University.

Transcardial perfusion and preparing of live brain slices

Before transcardial perfusion, the mouse was anesthetized with a gas mixture of oxygen and isoflurane (1.5–3%). Perfusion was carried out with an ice-cold solution of artificial cerebrospinal fluid (aCSF) No. 1 containing (in mM): 92 NMDG, 2.5 KCl, 1.2 NaH_2PO_4, 30 $NaHCO_3$, 20 HEPES, 25 D-glucose, 2 thiourea, 5 sodium

ascorbate, 3 sodium pyruvate, 0.5 $CaCl_2$, 10 $MgSO_4$, 6 N-acetylcysteine) (0–2°C, pH 7.3–7.4), aerated with carbogen (5% O_2 + 95% CO_2). After decapitation, the brain was quickly removed (followed by a removal of the cerebellum) and placed into an ice-cold solution of aCSF No. 1 for 1 min. The dorsal part of the brain was attached with cyanoacrylate adhesive to a special support and placed into ice-cold carbogen-saturated aCSF No. 1 for further slicing.

Horizontal hippocampal slices were obtained on a Leica VT1200 microtome with an amplitude of 1 cm, at a rate of 0.8 mm/s, in the dorsoventral plane. The thickness of slices for recording long-term potentiation (LTP) was 400 μm. Next, a hippocampal area was excised from the slice with a scalpel and transferred into aCSF No. 1 at room temperature. After 10 min, the hippocampal slices were transferred to a water bath for incubation at 34°C for 30 min. After 30 minutes, the slices were incubated for 1 h in aCSF No. 2 containing (in mM) 92 NaCl, 2.5 KCl, 1.2 NaH_2PO_4, 30 $NaHCO_3$, 20 HEPES, 25 D-glucose, 2 thiourea, 5 sodium ascorbate, 3 sodium pyruvate, 2 $CaCl_2$, 2 $MgSO_4$, 6 N-acetylcysteine) (0–2°C, pH 7.3–7.4) and saturated with carbogen at room temperature. After incubation, local field excitatory postsynaptic potentials (fEPSP) were recorded.

Method of extracellular electrophysiological recording

To study the mechanisms of synaptic plasticity in hippocampal slices of WT and YAC128 mice, an electrophysiological method based on the LTP phenomenon was used. Before the onset of fEPSP recording session, the slices were transferred into a special bath filled with a carbogen-saturated aCSF No. 3 containing (in mM) 124 NaCl, 2.5 KCl, 1.2 NaH_2PO_4, 24 $NaHCO_3$, 5 HEPES, 12.5 D-glucose, 2 $CaCl_2$, 2 $MgSO_4$), with a constant flow (5 mL/min) and a temperature of 32°C, and incubated for 20 min. In the experiment, 5–6 slices from each mouse were used. A stimulating bipolar electrode (double-twisted insulated nichrome wire 50 μm in diameter (A-M Systems, USA)) and a recording glass microelectrode were used to record fEPSP and induce LTP. A stimulating bipolar electrode was placed at the border of the hippocampal CA1 and CA2 areas along the Schaffer collaterals, while a recording electrode filled with aCSF No. 3 was placed in the CA1 area. fEPSP were recorded via a Multiclamp 700B amplifier (Molecular Device, USA) and Digidata 1440A digital-to-analog converter (Molecular Devices, USA) using MultiClamp Commander and pClamp 10.7 software (Axon Instruments, USA). Recording fEPSP before LTP induction was carried out every 20 s with paired-pulse electrical stimulation with a pulse duration of 0.1 ms and a 50-ms interstimulus interval. Electrical pulses were used in the range of 25 to 300 μA. The strength of electrical stimulation was selected as follows. Electrical stimulation of the slice was performed from a zero current value with a gradual increase in the current strength by 10-μA steps until the appearance of a kink in the descending fEPSP phase or a population spike. The final stimulation current was by 10 μA (this value was equal to the step whereby the current strength was selected) less than the current at which a population spike or a kink in the descending fEPSP phase appeared. With the current thus selected, the baseline was recorded (before fEPSP induction), and LTP was induced.

Before LTP induction, fEPSP were recorded for 20 min (baseline). In this case, the induction of LTP was started only if the dependence of the fEPSP slope angle on the strength of electrical stimulation changed by no more than 10% of the initial value. LTP was induced by a high-frequency electrical stimulation (HFS): 100 pulses for 1 s with two repeats every 200 ms. Following HFS, fEPSP were recorded for 60 min. To assess postsynaptic potentiation in the slice, the normalized values of the slope angle were averaged during the first 3 min after HFS. The normalized values of the slope angle were calculated as the ratio of the slope angle after LTP induction to the average slope angle of the baseline.

Preparation of the fixed brain slices and morphological analysis of dendritic spines

For visualization of the spines morphology with confocal microscope and their further analysis, YAC128 mice were cross-bred with Tg(Thy1-EGFP)MJrs/J mice (M strain). In M mice, solitary brain neurons express a green fluorescent

protein (GFP), which makes it possible to highlight contrastingly the body and processes of individual hippocampal neurons. As a result of crossbreeding, a hybrid of the two strains was obtained, which was then crossed with an M strain mouse within the same background. Animals of the 4th and 5th generations made up the experimental groups. A total of 4 groups were formed from mice of both genotypes aged 6 and 9 months (5 mice per group). To obtain fixed sections of the brain, the animals were anesthetized with urethane (250 mg/mL diluted in 0.9% sodium chloride solution), transcardially perfused with 4% paraformaldehyde diluted in phosphate-buffered saline (PBS, pH 7.2). Fixed sections were prepared on a microtome (Campden Instruments Ltd.). The average number of images for each dendritic fragment was 35–40 micrographs. A Z stack of optical sections of hippocampal neuron dendrites were taken with a ThorLabs confocal microscope with following parameters: Olympus UPlanSApo ×100 objective, resolution 1024 × 1024, section thickness 0.2 μm/pixel, thickness of a series of sections 4–5 μm. No less than 10 micrographs were taken for each mouse; with dendritic fragments at least 40 μm long, at a distance of 50 μm from the neuron body. The images were further processed in the Imaris software package. Based on the resulting images, a "blind" analysis of the morphology and the number of dendritic spines on the secondary apical dendrites of CA1 neurons was performed by the NeuronStudio software package. The spines were categorized according to the following parameters: minimum stubby spine size—10, non-stubby spine size—10, head-to-neck ratio—1.1, thin spine aspect ratio—2.5, mushroom spine size—0.3.

Morris water maze behavioral test

To study spatial memory, the Morris water maze was used. Platform-finding navigation of a mouse was carried in a round polypropylene pool (diameter 1.5 m) filled with water (21–23°C), aided by four black-and-white landmarks located outside the pool and oriented on the cardinal direction. During a 5-day behavioral test, the mouse, using the above landmarks, tried to find a platform submerged in opaque water for 90 s. Each training session, conducted at a daily basis and at the same time, consisted of 4 trials (attempts) separated by at least 15-min intervals. On day 5, only a single trial in the absence of the platform was carried out, also for 90 s. The animal's track was recorded by a VS 1304-1 video system using the Gigabit Ethernet interface and analyzed with the Minopontikos program [14]. The following test parameters were determined: the percentage of time spent on the test day in the quadrant, where the platform was previously located and the number of platform crossings. The number of successful platform-finding attempts during training sessions was also counted.

Statistical analysis

The Shapiro-Wilk test was used to check the experimental samples for normal distribution. If the groups demonstrated homogeneity of variance, the significance of differences between the two samples was revealed by the Student's *t*-test and by one-way ANOVA followed by the Tukey's post hoc test in case of several samples. In the case of data distribution other than normal, the Mann–Whitney *U*-test was used to reveal differences between two samples; for several samples, the Kruskal–Wallis test and the Benjamini–Yekutieli method were applied. The results were considered statistically significant at $p < 0.05$.

RESULTS

1. Impairment of long-term potentiation in a Huntington's disease mouse model

To reveal impairments in synaptic plasticity in HD mouse model, LTP values were measured in live hippocampal slices of control (WT) and experimental groups (HD model, YAC128 strain) at the age of 4 and 6 months. Comparisons were drawn between animals of the same age. In 4-month-old animals impaired synaptic plasticity was found in YAC128 mice: LTP values were 2.24 ± 0.22 and 1.53 ± 0.15 in WT vs. YAC128 mice respectively (Mann–Whitney test, $p < 0.05$; Fig. 1a). In 6-month-old animals impaired LTP were also confirmed in HD mice (Fig. 1b). In WT mice, the mean LTP was 1.75 ± 0.13, which is significantly different from the value recorded in

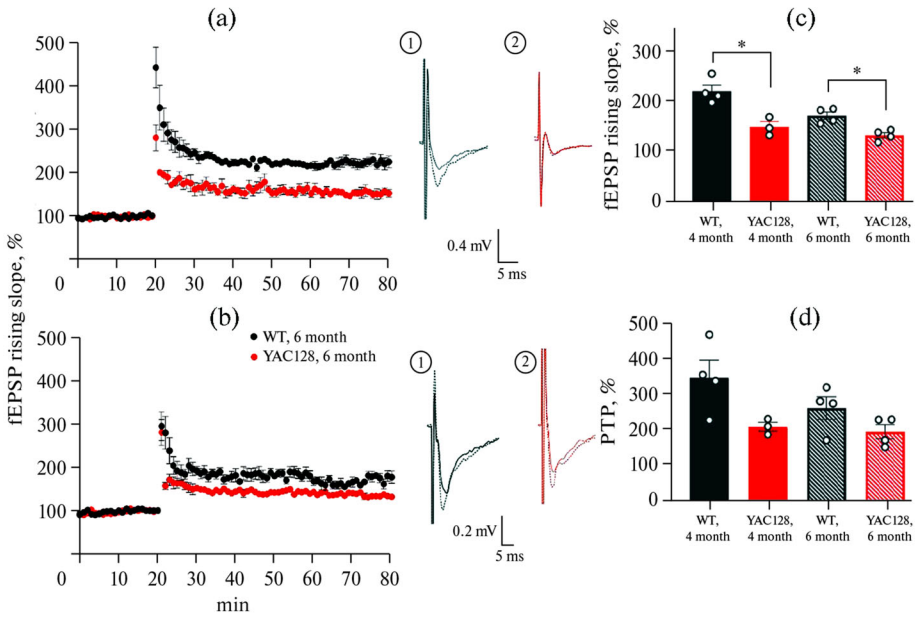

Fig. 1. Long-term potentiation is attenuated in the CA1 field of the hippocampus in the HD mouse model at the age of 4 and 6 months. (a) Representative recordings and the normalized value of the slope of the fEPSP before (marked with a solid line) and after (marked with a dashed line) high-frequency stimulation in WT mice ($n = 4$) and YAC128 mice ($n = 3$) at the age of 4 months. (b) Representative recordings and the normalized value of the slope of the fEPSP before (marked with a solid line) and after (marked with a dashed line) high-frequency stimulation in WT mice ($n = 4$) and YAC128 mice ($n = 4$) at the age of 6 months. (c) Diagram illustrating the differences in the value of LTP between wild-type mice and the HD mouse model at the age of 4 and 6 months. Data are presented as mean ± SEM, * $p < 0.05$, significance was calculated using the Mann–Whitney test. (d) Diagram illustrating the PTP values between WT and the HD mouse model at the age of 4 and 6 months. Data are presented as mean ± SEM.

YAC128 mice (1.35 ± 0.09) (Mann–Whitney test, $p < 0.05$). The results are shown in Fig. 1c as diagrams illustrating a change in the LTP value after HFS in control and experimental groups of mice at the age of 4 and 6 months. In addition, post-tetanic potentiation (PTP) was evaluated in different age groups of both strains. At the age of 4 months, despite the fact that no statistically significant differences were found, there was a downward trend in PTP values, as tracked in mice with an HD model compared to WT animals: 3.49 ± 0.43 and 2.11 ± 0.1, respectively. At 6 months, no statistically significant differences in the PTP value in both strains were detected: 2.6 ± 0.3 and 1.97 ± 0.17 in WT vs. YAC128 mice respectively (Fig. 1d).

2. Morphological changes in dendritic spines of CA1 hippocampal neurons in Huntington's disease mouse model

To study the morphology of neuronal dendritic spines, a new transgenic mouse strain, YAC128-M, was obtained. In this strain, in addition to mHTT, single neurons in different parts of the brain, including hippocampus, single neurons expressed GFP controlled by a neuron-specific promoter Thy1. This strain simplifies visualization the structure of neurons for further morphological analysis of dendritic trees. Importantly, the presence of the transgenic insertion did not affect the level of GFP fluorescence in the HD mice (Fig. 2a).

To evaluate the morphological differences in dendritic spines of CA1 hippocampal neurons, a series of micrographs of dendritic fragments was obtained in mice at the aged of 6 and 9 months. At the age of 6 months, significant differences were observed in the density of dendritic spines in WT vs. transgenic mice (WT: 9.3 ± 0.3 per 10 μm; YAC128: 10.9 ± 0.3 per 10 μm; $p < 0.001$; Fig. 2b). An increase in the number of mushroom dendritic spines made a largest contribution to this difference (WT: 41.8 ± 1.3%; YAC128: 47.5 ± 1.4%; $p = 0.03$). However, by the age of

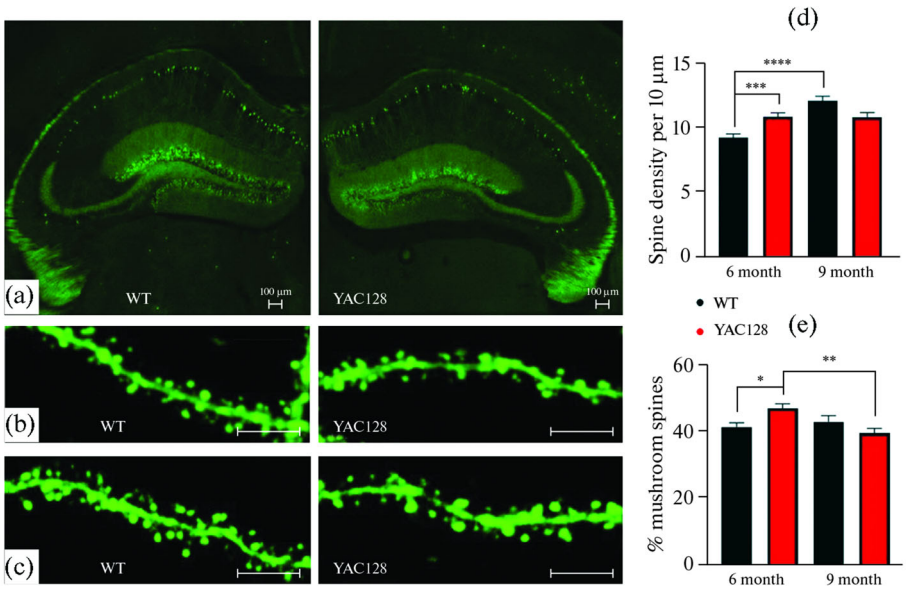

Fig. 2. Changes in the morphology and number of postsynaptic dendritic spines in the HD mouse model. (a) Expression of green fluorescent protein in hippocampal neurons on brain slices of WT and YAC128 mice crossed with M mice. Confocal microscopy, ×4. Scale bar length corresponds to 100 μm. (b) Micrographs of dendritic tree fragments and histograms illustrating the number of dendritic spines of CA1 neurons in the hippocampal region of WT and YAC128 mice at the age of 6 months. Confocal microscopy, ×100. Scale bar, 10 μm. (c) Micrographs of dendritic tree fragments and histograms illustrating the morphology of dendritic spines of CA1 neurons in the hippocampal region of WT and YAC128 mice at the age of 9 months. Confocal microscopy, ×100. Scale bar, 10 μm. (d) Histogram illustrating the density of dendritic spines of CA1 neurons in the hippocampal region of WT and YAC128 mice at the age of 6 and 9 months, Data are presented as mean ± SEM, *** $p < 0.005$. (e) Histogram illustrating the number of mushroom dendritic spines of CA1 neurons in the hippocampal region of WT and YAC128 mice at the age of 6 and 9 months, Data are presented as mean ± SEM, **** $p < 0.001$.

9 months, the density of dendritic spines in CA1 neurons of WT mice turned out to be higher than in HD mouse model (WT: 12.1 ± 0.3 per 10 μm; YAC128: 10.9 ± 0.3 per 10 μm; $p = 0.01$; Fig. 2c). The number of mushroom dendritic spines in HD mice was insignificantly lower than in WT mice (WT: 43.3 ± 1.9%; YAC128: 40 ± 1.4%, YAC128 at 9 months: 47.4 ± 1.3%; $p = 0.15$). With age, in CA1 neurons of WT mice, there was an upward trend in the density of dendritic spines (WT at 6 months: 9.2 ± 0.3 per 10 μm; WT at 9 months: 12.1 ± 0.3 per 10 μm; $p = 0.0001$), while in animals with HD, this parameter remained unchanged (YAC128 at 6 months: 10.9 ± 0.3 per 10 μm; YAC128 at 9 months: 10.9 ± 0.3 per 10 μm; $p = 0.9$) (Fig. 2d). In addition, the number mushroom spines in transgenic mice at the age of 9 months was reduced compared to the same parameter in younger animals of the same genotype (YAC128 at 6 months: 47.4 ± 1.3%; YAC128 at 9 months: 40 ± 1.4%; $p = 0.004$) (Fig. 2e).

3. Impairments in spatial memory formation in Huntington's disease mouse model

To analyze cognitive impairments in HD mice, the most common test—Morris water maze, was used to assess the hippocampus-associated impairments in memory formation, including the acquisition of new skills and memorization. Figures 3a, 3b show the tracks of WT and YAC128 mice at the age of 6 and 9 months on the test day.

On the test day 6-month-old WT and YAC128 mice, on average spent the equal amount of time in the quadrant where the platform was located during training (28.0 ± 5.1% and 21.6 ± 4.2%) (Fig. 3c). We also calculated the number of crossings of the area where the platform was located during the training sessions. WT mice crossed this area on average more often (the number of crossings on the test day was 1.81 ± 0.5) than transgenic mice for which this parameter was 1 ± 0.4, but also didn't reached statistically significant values (Fig. 3e). Next, we analyzed the learning abil-

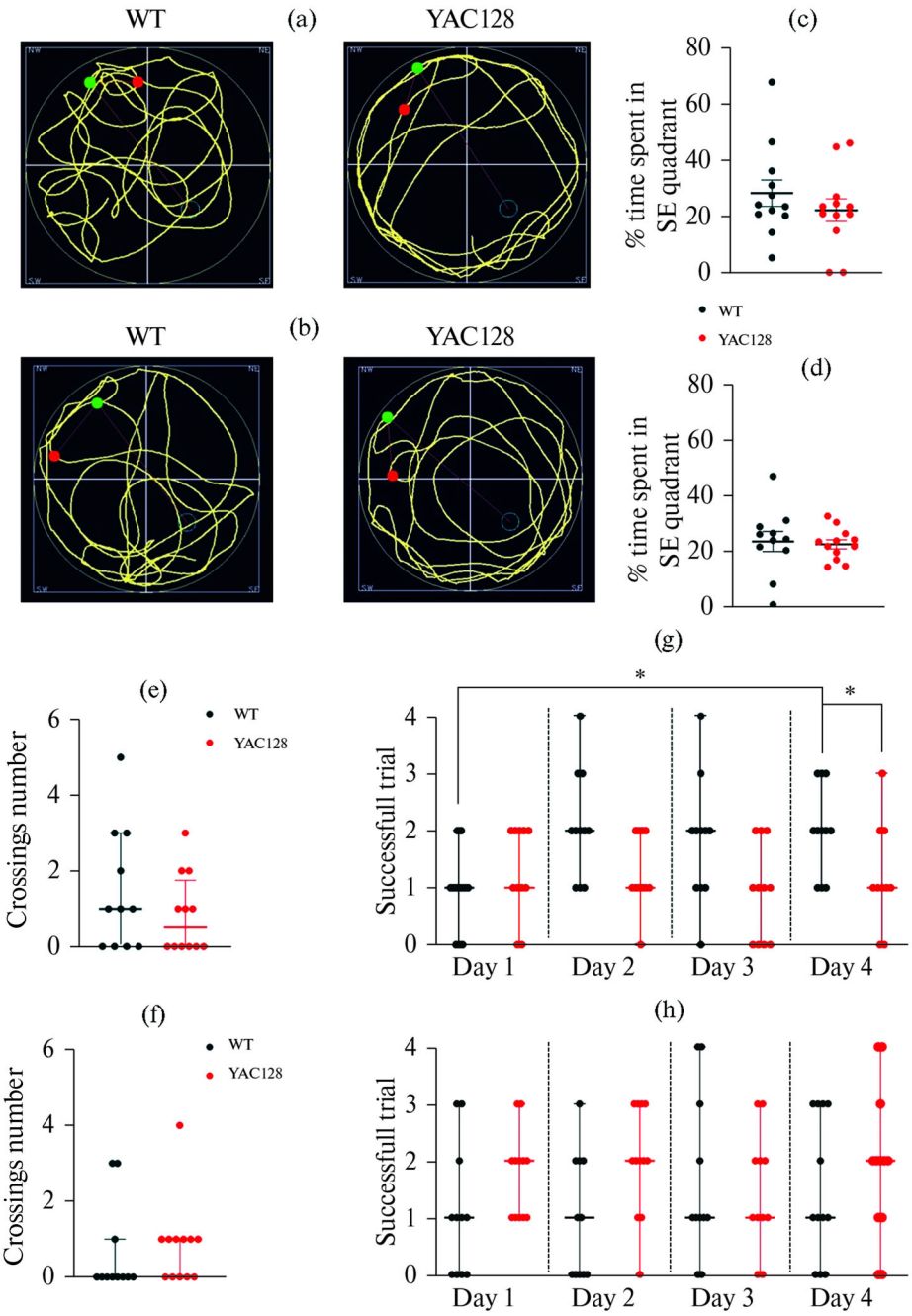

Fig. 3. Impairments in the formation of spatial memory in the HD mouse model. (a) Trajectory of movement of WT mice (n = 11) and YAC128 mice (n = 11) in the pool on the test day at the age of 6 months. (b) Trajectory of movement of WT mice (n = 12) and YAC128 mice (n = 10) in the pool on the test day at the age of 9 months. (c) A graph illustrating the individual values of the percentage of time for WT and YAC128 mice at the age of 6 months spent in the SE quadrant on the test day, where the hidden platform was located during training. Data are presented as mean ± SEM. (d) A graph illustrating the individual values of the percentage of time for WT and YAC128 mice at the age of 9 months spent in the SE quadrant on the test day, where the hidden platform was located during training. Data are presented as mean ± SEM. (e) A graph illustrating the number of platform crossings on the test day for WT and YAC128 mice at the age of 6 months. Data are presented as median ± interquartile range. (f) A graph illustrating the number of platform crossings on the test day for WT and YAC128 mice at the age of 9 months. Data are presented as median ± interquartile range. (g) A graph illustrating the individual number of successful platform-finding attempts on each training day for WT and YAC128 mice at the age of 6 months. Data are presented as median ± interquartile range. (h) A graph illustrating the individual number of successful platform-finding attempts on each training day for WT and YAC128 mice at the age of 9 months. Data are presented as median ± interquartile range.

ity of mice by accessing the number of successful attempts to find the platform on days 1 and 4. By the end of the training sessions, WT mice coped with platform finding more successfully and found it on average in half of the attempts, while the number of successful attempts in HD mouse model was noticeably lower than in WT mice, averaging a single successful attempt ($p = 0.04$). The number of successful attempts on training day 1 was the same in mice of both genotypes and consisted of one attempt. Thus, WT mice demonstrated the ability to learn and memorize new information progressing with the number of successful attempts from one to two by training day 4 ($p = 0.02$), while in YAC128 mice, the number of successful attempts remained the same on both day 1 and day 4 (Fig. 3g).

By the age of 9 months, the learning ability in mice of both genotypes generally decreased as they spent on average the same amount of time in the quadrant, where the platform was located during training sessions (24.16 ± 3.6% and 23.14 ± 1.7% for WT vs. YAC128 mice, respectively) (Fig. 3d). On the test day, the number of crossings of the area, where the platform was previously located, was also statistically indistinguishable, amounting to 0.72 ± 0.3 and 1 ± 0.3 for WT vs. YAC128 mice, respectively (Fig. 3f). When assessing the number of successful platform-finding attempts, no differences were also found between both genotypes and mice of the same genotype on training days 1 and 4; their number was one and two for WT and YAC128 mice, respectively (Fig. 3h).

DISCUSSION

It has been generally accepted for a long time that cognitive dysfunction in HD patients is caused by pathological changes in the corticostriatal pathway, as evidenced by the data obtained both on murine models and in studies with HD patients [15]. However, in some studies, it has been noted that *mHtt*-associated pathological processes in the hippocampus may contribute to the development of cognitive dysfunction. This is evidenced by the progressive age-related accumulation of mHTT in the nuclei of hippocampal neurons resulting in the formation of neuronal intranuclear inclusions [16, 17]. In addition, this hypothesis is supported by experimental studying of the LTP mechanisms in the hippocampus of HD animal models. LTP represents an enhancement in synaptic transmission between two neurons, which persists for a long time after the end of stimulation. According to the concept of modern neurobiology, this process underlies the cellular mechanisms of memory and learning. Impaired LTP mechanisms in the hippocampus of HD mouse models were first reported by Usdin et al. [18]. Further studies showed the relationship between reduced LTP and the behavioral phenotype expressed in impaired spatial cognition [19], and these impairments occurred before the death of neurons. Subsequently, this phenomenon was described in various HD models, including the transgenic (knock-in) Hu97/18 mouse model of HD [20], which is unique in that it only contains the human huntingtin gene. In brain slices of Hu97/18 mice at the age of 9 months, the authors found a complete lack of LTP 50–60 min after HFS, which is consistent with the data described by another authors [18, 19, 21]. While at the age of 3 months, LTP was shown to be unimpaired [22], thus indicating that cognitive impairments in the Hu97/18 model are progressive. In our LTP study at the age of 4 months, we also observed a decrease in the magnitude of synaptic plasticity after HFS in HD mice compared to WT mice. At the age of 6 months, the difference in LTP between the two genotypes was also observed.

Morphological changes in hippocampal neurons in HD reflect functional changes. As in other neurodegenerative diseases, in HD, the structure of the neuronal dendritic tree, especially dendritic spines has changed [13]. The spines are highly dynamic postsynaptic structures; hence, changes in their morphology reflect functional alterations that occur in a synapse during synaptic transmission. The density and morphology of the dendritic spines closely correlate with the activity of many cellular processes, some of which are involved in the mechanisms of synaptic plasticity regulation, which, in turn, represents a substrate of such cognitive functions as learning and memory [23]. Elimination of the spines leads to the loss of synaptic connections between neurons and underlies

the cellular mechanisms of cognitive impairments. Previously, morphological analysis of the apical dendrites in hippocampal CA1 pyramidal neurons was only carried out in the R6/2 transgenic mouse model of HD, having shown a decrease in the density of dendritic spines, mainly due to a decrease in the fraction of mushroom spines compared to the control group. Moreover, the authors noted an increase in the number of filopodia-like structures in the same mouse model HD [24]. Studies of the morphology of dendritic spines were also carried out on cultured hippocampal neurons. It was demonstrated that the mushroom dendritic spines are more susceptible to elimination nearby mHTT aggregates than other spine types [25]. However, in YAC128 mice, aggregates of mutant huntingtin appear only at the age of 12 months [2] and, therefore, are unable to exert a negative impact on morphofunctional changes in synapses. In our study, we first observed an increase in the density of dendritic spines and the number of mushroom spines in YAC128 mice compared to WT mice aged 6 months, which was followed by a gradual decrease in the density of spines by the age of 9 months; and this decrease cannot be explained by mHTT aggregation, which is not yet observed in the hippocampus at this age. The previous analysis of the electrophysiological activity of nerve cells revealed an increased release of glutamate from the axonal terminals of cortical neurons, which was recorded in this model [26]. Experiments on studying the colocalization of pre- and postsynaptic marker proteins VGLUT1 and GluA2 respectively also demonstrated an increase in mushroom spines in cultured cortical neurons isolated from YAC128 mice [27]. Another explanation for the results of these studies may arise from the normal function of the HTT protein, which normally enhances the expression of the brain-derived neurotrophic factor (BDNF). In addition to the gene encoding its own HTT, the genome of transgenic mice contains the human HTT gene. Therefore, in the presymptomatic period, an increased BDNF level can lead to an increase in the fraction of mushroom spines, an important role in maintaining the structure of which belongs to BDNF. However, the BDNF level decreases with the progression of neuropathology, as was previously shown in an article describing the relationship between structural changes in dendritic spines and impaired synaptic plasticity in the hippocampus of HD mice [21]. As noted above, the morphology of synapses closely correlates with their functional activity; therefore, a decrease in the BDNF level in HD led eventually to a decrease in actin polymerization, the main biochemical process responsible for the structural organization of the dendritic spine's cytoskeleton.

Spatial memory impaired due to mHTT aggregation in R6/2 mice was detected before than other behavioral changes [28]. YAC128 mice aged 8 months also exhibit impairments of spatial memory, as revealed in a simplified swimming test differing from the Morris water maze test in the small size of the pool and the test time. In Hu97/18 mice, spatial learning detected in the test for recognition of a known object in a novel location was also deteriorates. In this test, the HD mice exhibited impaired spatial learning since the age of 6 months [22].

In HD patients, hippocampus-associated dysfunction in spatial orientation were also identified using a virtual pool divided into four quadrants, in which a hidden platform was to be found. According to epy data, in the premanifest period, the control group and that of patients with HD spent on average most of the time of platform finding in the correct quadrant, while patients with an early stage of HD spend far less time in the correct quadrant, suggesting a random search scheme. Besides, during the study, subjects also executed a paired associates test intended to assess visual and associative memory. This test is used to diagnose Alzheimer's disease and activates the hippocampal region, as shown by functional magnetic resonance imaging. Patients with an early stage of HD made mistakes much more frequently than healthy volunteers. In addition, in the premanifest period, HD patients made 3 times more errors in tasks with 6 and 8 samples, with the error rate correlating with the estimated time before disease manifestation [29]. In our study, we also observed impairment in spatial memory formation, beginning from the age of 6 months. Although, on the test day, differences were found neither in the percentage of time nor in the number of platform

area crossings, WT mice, in general, performed better in finding the platform by the end of training sessions, while HD mice were unable to memorize new information and did not improve their parameters by the end of training sessions, which well correlates with the decrease in synaptic plasticity observed at this age.

Thus, our data point out to the neurodegenerative changes in the hippocampus in the development of cognitive impairments observed in HD mice. The observed hippocampal impairments contribute to systemic synaptic dysfunction in HD neuropathology in different brain regions, which occurs even in the absence of mutant protein aggregates in neurons.

AUTHORS' CONTRIBUTION

Conceptualization and experimental design (N.A.K., A.I.E., I.B.B.); data collection (N.A.K., A.I.E., E.D.G., S.A.P., G.E.I.); data processing (N.A.K., A.I.E., E.D.G., S.A.P., G.E.I.); writing and editing the manuscript (N.A.K., A.I.E., O.L.B., I.B.B.).

FUNDING

This work was supported by the Russian Science Foundation (RSF, grant No. 19-15-00184) and the Ministry of Science and Higher Education of the Russian Federation within the World-Class Research Center (WCRC) program "Advanced digital technologies" (treaty No. 075-15-2020-934 of November 17, 2020) in the following proportion: experiments illustrated in Figs. 1, 2b–2e were supported by the RSF; the experiment in Fig. 2a was financed by the WCRC program.

CONFLICT OF INTEREST

The authors declare that they have neither evident nor potential conflict of interest related to the publication of this article.

REFERENCES

1. The Huntington's Disease Collaborative Research Group (1993) A novel gene containing a trinucleotide repeat that is expanded and unstable on Huntington's disease chromosomes. Cell 72: 971-983. https://doi.org/10.1016/0092-8674(93)90585-e
2. Van Raamsdonk JM, Warby SC, Hayden MR (2007) Selective degeneration in YAC mouse models of Huntington disease. Brain Res Bull 72: 124-131. https://doi.org/10.1016/j.brainresbull.2006.10.018
3. Van Raamsdonk JM, Pearson J, Slow EJ, Hossain SM, Leavitt BR, Hayden MR (2005) Cognitive dysfunction precedes neuropathology and motor abnormalities in the YAC128 mouse model of Huntington's disease. J Neurosci 25: 4169-4180. https://doi.org/10.1523/JNEUROSCI.0590-05.2005
4. Lichter DG, Hershey LA (2010) Before chorea: pre-Huntington mild cognitive impairment. Neurology 75: 490-491. https://doi.org/10.1212/WNL.0b013e3181ec805b
5. Lawrence AD, Hodges JR, Rosser AE, Kershaw A, French-Constant C, Rubinsztein DC, Robbins TW, Sahakian BJ (1998) Evidence for specific cognitive deficits in preclinical Huntington's disease. Brain 121 (Pt 7): 1329-1341. https://doi.org/10.1093/brain/121.7.1329
6. Nithianantharajah J, Hannan A (2013) Dysregulation of synaptic proteins, dendritic spine abnormalities and pathological plasticity of synapses as experience-dependent mediators of cognitive and psychiatric symptoms in Huntington's disease. Neuroscience 251: 66-74. https://doi.org/10.1016/j.neuroscience.2012.05.043
7. Tonnesen J, Nagerl UV (2016) Dendritic Spines as Tunable Regulators of Synaptic Signals. Front Psychiatry 7: 101. https://doi.org/10.3389/fpsyt.2016.00101
8. Wu J, Ryskamp DA, Liang X, Egorova P, Zakharova O, Hung G, Bezprozvanny I (2016) Enhanced Store-Operated Calcium Entry Leads to Striatal Synaptic Loss in a Huntington's Disease Mouse Model. J Neurosci 36: 125-141. https://doi.org/10.1523/JNEUROSCI.1038-15.2016
9. Cepeda C, Hurst RS, Calvert CR, Hernandez-Echeagaray E, Nguyen OK, Jocoy E, Christian LJ, Ariano MA, Levine MS (2003) Transient and progressive electrophysiological alterations in the corticostriatal pathway in a mouse model of Huntington's disease. J Neurosci 23: 961-969. https://doi.org/10.1523/JNEUROSCI.23-03-00961.2003
10. Indersmitten T, Tran CH, Cepeda C, Levine MS (2015) Altered excitatory and inhibitory inputs to

striatal medium-sized spiny neurons and cortical pyramidal neurons in the Q175 mouse model of Huntington's disease. J Neurophysiol 113: 2953-2966. https://doi.org/10.1152/jn.01056.2014

11. Murmu RP, Li W, Holtmaat A, Li JY (2013) Dendritic spine instability leads to progressive neocortical spine loss in a mouse model of Huntington's disease. J Neurosci 33: 12997-13009. https://doi.org/10.1523/JNEUROSCI.5284-12.2013
12. Schmidt ME, Buren C, Mackay JP, Cheung D, Dal Cengio L, Raymond LA, Hayden M (2018) Altering cortical input unmasks synaptic phenotypes in the YAC128 cortico-striatal co-culture model of Huntington disease. BMC Biol 16: 58. https://doi.org/10.1186/s12915-018-0526-3
13. Spires TL, Grote HE, Garry S, Cordery PM, Van Dellen A, Blakemore C, Hannan AJ (2004) Dendritic spine pathology and deficits in experience-dependent dendritic plasticity in R6/1 Huntington's disease transgenic mice. Eur J Neurosci 19: 2799-2807. https://doi.org/10.1111/j.0953-816X.2004.03374.x
14. Chernyuk DP, Zorin AG, Derevtsova KZ, Efimova EV, Prikhodko VA, Sysoev YI, Vlasova OL, Bolsunovskaia MV, Bezprozvanny IB (2021) Automatic analysis of the "Morris water maze" behavioral test data. Zhurn Vysshei Nervn Deyatelnosti Im IP Pavlova 71: 126-135. https://doi.org/10.31857/S0044467721010044
15. Montoya A, Price BH, Menear M, Lepage M (2006) Brain imaging and cognitive dysfunctions in Huntington's disease. J Psychiatry Neurosci 31: 21-29.
16. Milnerwood AJ, Cummings DM, Dallerac GM, Brown JY, Vatsavayai SC, Hirst MC, Rezaie P, Murphy KP (2006) Early development of aberrant synaptic plasticity in a mouse model of Huntington's disease. Hum Mol Genet 15: 1690-1703. https://doi.org/10.1093/hmg/ddl092
17. Paldino E, Giampa C, Montagna E, Angeloni C, Fusco FR (2019) Modulation of Phospho-CREB by Systemically Administered Recombinant BDNF in the Hippocampus of the R6/2 Mouse Model of Huntington's Disease. Neurosci J 2019: 8363274. https://doi.org/10.1155/2019/8363274
18. Usdin MT, Shelbourne PF, Myers RM, Madison DV (1999) Impaired synaptic plasticity in mice carrying the Huntington's disease mutation. Hum Mol Genet 8: 839-846. https://doi.org/10.1093/hmg/8.5.839
19. Murphy KP, Carter RJ, Lione LA, Mangiarini L, Mahal A, Bates GP, Dunnett SB, Morton AJ (2000) Abnormal synaptic plasticity and impaired spatial cognition in mice transgenic for exon 1 of the human Huntington's disease mutation. J Neurosci 20: 5115-5123. https://doi: 10.1523/JNEUROSCI.20-13-05115.2000
20. Kolodziejczyk K, Parsons MP, Southwell AL, Hayden MR, Raymond LA (2014) Striatal synaptic dysfunction and hippocampal plasticity deficits in the Hu97/18 mouse model of Huntington disease. PLoS One 9: e94562. https://doi.org/10.1371/journal.pone.0094562
21. Lynch G, Kramar EA, Rex CS, Jia Y, Chappas D, Gall CM, Simmons DA. (2007) Brain-derived neurotrophic factor restores synaptic plasticity in a knock-in mouse model of Huntington's disease. J Neurosci 27: 4424-4434. https://doi.org/10.1523/JNEUROSCI.5113-06.2007
22. Southwell AL, Warby SC, Carroll JB, Doty CN, Skotte NH, Zhang W, Villanueva EB, Kovalik V, Xie Y, Pouladi MA, Collins JA, Yang XW, Franciosi S, Hayden MR (2013) A fully humanized transgenic mouse model of Huntington disease. Hum Mol Genet 22: 18-34. https://doi.org/10.1093/hmg/dds397
23. McCann RF, Ross DA (2017) A Fragile Balance: Dendritic Spines, Learning, and Memory. Biol Psychiatry 82: e11-e13. https://doi.org/10.1016/j.biopsych.2017.05.020
24. Bulley SJ, Drew CJ, Morton AJ (2012) Direct Visualisation of Abnormal Dendritic Spine Morphology in the Hippocampus of the R6/2 Transgenic Mouse Model of Huntington's Disease. J Huntingtons Dis 1: 267-273. https://doi.org/10.3233/JHD-120024
25. Richards P, Didszun C, Campesan S, Simpson A, Horley B, Young KW, Glynn P, Cain K, Kyriacou CP, Giorgini F, Nicotera P (2011) Dendritic spine loss and neurodegeneration is rescued by Rab11 in models of Huntington's disease. Cell Death Differ 18: 191-200. https://doi.org/10.1038/cdd.2010.127
26. Koch ET, Woodard CL, Raymond LA (2018) Direct assessment of presynaptic modulation of cortico-striatal glutamate release in a Huntington's disease mouse model. J Neurophysiol 120: 3077-3084. https://doi.org/10.1152/jn.00638.2018
27. Smith-Dijak AI, Nassrallah WB, Zhang LYJ, Geva M, Hayden MR, Raymond LA (2019) Impairment and Restoration of Homeostatic Plasticity in Cultured Cortical Neurons From a Mouse Model of Huntington Disease. Front Cell Neurosci 13: 209. https://doi.org/10.3389/fncel.2019.00209
28. Lione LA, Carter RJ, Hunt MJ, Bates GP, Mor-

ton AJ, Dunnett SB (1999) Selective discrimination learning impairments in mice expressing the human Huntington's disease mutation. J Neurosci 19: 10428-10437. https://doi: 10.1523/JNEUROSCI.19-23-10428.1999

29. Begeti F, Schwab LC, Mason SL, Barker RA (2016) Hippocampal dysfunction defines disease onset in Huntington's disease. J Neurol Neurosurg Psychiatry 87: 975-981. https://doi.org/10.1136/jnnp-2015-312413

Translated by A. Polyanovsky